

Extended paraconductivity regime in underdoped cuprates

S. Caprara,¹ M. Grilli,¹ B. Leridon,² and J. Lesueur²

¹*Istituto Nazionale per la Fisica della Materia, Unità di Roma 1 and SMC Center, and Dipartimento di Fisica Università di Roma “La Sapienza”, piazzale Aldo Moro 5, I-00185 Roma, Italy*

²*Laboratoire de Physique Quantique—ESPCI/UPR5-CNRS, 10, Rue Vauquelin, 75005 Paris, France*

(Received 19 April 2005; revised manuscript received 22 July 2005; published 13 September 2005)

We reconsider transport experiments in strongly anisotropic high- T_c superconducting cuprates and we find that the universal Aslamazov-Larkin paraconductivity in two dimensions is surprisingly robust, even in the underdoped regime below the pseudogap crossover temperature T^* . We also establish that the underlying normal-state resistivity in the pseudogap region is (almost) linear in temperature, with all the deviations being quantitatively accounted for by Aslamazov-Larkin paraconductivity. The disappearance of paraconductivity is ruled by the suppression of Gaussian pair fluctuations at an energy scale related to T^* .

DOI: [10.1103/PhysRevB.72.104509](https://doi.org/10.1103/PhysRevB.72.104509)

PACS number(s): 74.72.-h, 74.25.Fy, 74.40.+k, 74.20.De

I. INTRODUCTION

Recent transport experiments^{1–3} in high- T_c superconducting cuprates have shown that the paraconductivity effects in the normal state above the critical temperature T_c are well described by the following expressions valid in two and three dimensions, respectively:

$$\Delta\sigma_{D=2}^{\text{exp}} = \frac{e^2}{16\hbar d \epsilon_0 \sinh(\epsilon/\epsilon_0)}, \quad (1)$$

$$\Delta\sigma_{D=3}^{\text{exp}} = \frac{e^2}{16\hbar \xi_{c0} \sqrt{2\epsilon_0} \sinh(2\epsilon/\epsilon_0)}, \quad (2)$$

where d is the distance between the CuO_2 layers, ξ_{c0} is the coherence length along the direction perpendicular to the layers, $\epsilon \equiv \log(T/T_c) \approx (T - T_c)/T_c$ is the dimensionless measure of the deviation from criticality, T is the temperature, and $\epsilon_0 \equiv \log(T^\# / T_c)$ is a dimensionless fitting parameter that is translated into a temperature scale $T^\#$ by analogy with ϵ . When the parameter ϵ_0 is adjusted to fit the experimental data, the corresponding temperature scale $T^\#$ turns out to increase with decreasing doping and appears to follow the characteristic crossover temperature T^* below which many different experiments in the cuprates reveal a pseudogap opening.⁴ The above expressions, Eqs. (1) and (2), and the experimental data that they fit well, display two remarkable features.

First of all, for temperatures T close to T_c , i.e., for small values of ϵ , they reproduce the Aslamazov-Larkin (AL) expression for the paraconductivity,⁵

$$\Delta\sigma_{D=2}^{\text{AL}} = \frac{e^2}{16\hbar d \epsilon}, \quad (3)$$

$$\Delta\sigma_{D=3}^{\text{AL}} = \frac{e^2}{32\hbar \xi_{c0} \sqrt{\epsilon}}. \quad (4)$$

These expressions account well for the fluctuating regime near T_c both in optimally doped and underdoped cuprates, with $\text{YBa}_2\text{Cu}_3\text{O}_{6+x}$ (YBCO) displaying three-dimensional fluctuations, whereas the other more anisotropic compounds,

$\text{La}_{2-x}\text{Sr}_x\text{CuO}_4$ (LSCO) and $\text{Bi}_2\text{Sr}_2\text{CaCu}_2\text{O}_{8+x}$ (BSCCO), have a two-dimensional behavior.

The fact that the paraconductivity in strongly anisotropic (quasi-two-dimensional) underdoped cuprates is described by “traditional” AL fluctuations is at odds with the widespread idea that, below the pseudogap formation temperature T^* , particle-particle pairs are formed, which only become phase coherent at the lower superconducting transition temperature T_c . According to this picture, below the temperature of pair formation the fluctuations would be vortex driven and should display a Kosterlitz-Thouless behavior, with exponential temperature dependences.

On the contrary, it seems a well-established experimental fact that the superconducting fluctuations in the more two-dimensional-like systems (essentially all, but the YBCO) display AL power-law behaviors in ϵ .^{6–11} Remarkably, in $D=2$ the AL theory of paraconductivity does not allow for any fitting parameter besides the experimentally well-accessible distance d between the two-dimensional CuO_2 layers, which translates the two-dimensional conductivity, with dimensions Ω^{-1} , in a three-dimensional conductivity with dimensions $\Omega^{-1} \text{m}^{-1}$. Therefore the AL paraconductive behavior observed near T_c strikingly shows that the establishment of superconducting phase coherence in these materials is *not due to a simple condensation of preformed pairs*. This by no means implies that preformed pairs are not present below T^* , but simply means that the superconducting coherence is driven by the formation of more loosely bound traditional BCS pairs. Various proposals have already been put forward based on the coexistence of fermionic quasiparticles (eventually forming BCS pairs at T_c) and preformed pairs with a more or less marked bosonic character.^{12–15}

The second remarkable feature of the experimental data described by Eqs. (1) and (2) regards the exponential suppression of the paraconductivity when $\epsilon > \epsilon_0$.¹⁶ While it is quite natural that superconducting fluctuations decay when moving away from T_c , no longer contributing to the conductivity, the fact that AL fluctuations are ruled by (and are suppressed above) a temperature scale related to T^* is surprising. In underdoped cuprates this rapid drop in the AL fluctuations occurring at the temperature scale $T^\# \sim T^*$, which is substantially higher than the superconducting tem-

perature T_c , implies a wide temperature range for superconducting fluctuations.

In principle, one could argue that T^* is indeed the temperature below which superconducting Cooper-pair fluctuations arise, and therefore it is not surprising that they contribute *à la* AL to the paraconductivity. However, upon underdoping, T^* increases, while T_c decreases. If this is interpreted within a standard scheme of strong-coupling pairing, the phase fluctuations would be (the only) responsible for paraconductivity, in $D=2$, and one should rather observe the Kosterlitz-Thouless-like condensation of preformed pairs. A recent calculation of the paraconductivity in the Gaussian-to-Kosterlitz-Thouless crossover regime¹⁷ produce a positive correction to the AL result, which is in disagreement with the experimentally observed monotonic suppression described by Eq. (1).

In this paper we focus on these two main features that emerge from the analysis of the paraconductivity measurements.

First, in Sec. II, we critically reexamine the AL theory and the possible occurrence of momentum and/or energy cutoffs in the critical pair fluctuations. This will provide a different perspective on the rapid drop of the paraconductivity above T^* , with respect to previous works,^{18,19} but will leave open the question of the mechanism allowing for the long survival of AL fluctuations in the pseudogap region of underdoped cuprates.

Then, in Sec. III, we focus on the two-dimensional materials and examine the robustness of the AL paraconductivity at various doping upon varying the assumed normal-state resistivity. Again, our scope is neither to provide a microscopic theory for the normal state and its collective excitations, nor to provide a theory for the interplay between normal-state and pair fluctuations below T^* . Our main concern here is rather to extract the most likely form of the normal-state resistivity in connection to the distinct presence of paraconductivity. We concentrate our attention on the two-dimensional case because the universal form of AL paraconductivity renders this analysis more stringent.

Concluding remarks are found in Sec. IV.

II. PARACONDUCTIVITY SUPPRESSION AROUND T^*

We discuss the paraconductivity starting by revisiting the derivation of the standard AL result in D spatial dimensions,^{5,20}

$$\Delta\sigma_D^{\text{AL}} = \alpha_D \int \frac{d^D\mathbf{q}}{(2\pi)^D} q^2 \mathcal{I}(\Omega_{\mathbf{q}}; T), \quad (5)$$

where α_D is a prefactor that acts as a coupling constant of the collective pair fluctuations with the electromagnetic field and is related to the fermion loops in the diagrammatic approach^{5,20} calculated at zero external frequency (these fermion loops also contribute with the q^2 factor) and

$$\mathcal{I}(\Omega_{\mathbf{q}}; T) \equiv \int_{-\infty}^{+\infty} \frac{dz}{\pi} \frac{z^2}{(z^2 + \Omega_{\mathbf{q}}^2)^2} \left(-\frac{\partial b(z)}{\partial z} \right). \quad (6)$$

Here $\Omega_{\mathbf{q}}$ is the inverse relaxation time of the collective pair fluctuations with a wave vector \mathbf{q} , which at low momenta

takes the hydrodynamic form $\Omega_{\mathbf{q}} \approx m + \nu q^2$ with a “mass” term $m \propto T \log(T/T_c) \propto T - T_c$ measuring the distance from criticality, and a characteristic inverse time scale ν ; $b(z) = [e^{z/T} - 1]^{-1}$ is the Bose distribution at a temperature T (in energy units). Here and in the following $q \equiv |\mathbf{q}|$, we take $\hbar = 1$, and measure lengths and inverse wave vectors in units of the lattice spacing a .

The inverse relaxation time $\Omega_{\mathbf{q}}$ is often referred to as the energy of the collective pair fluctuations. Although this terminology is improper, as the dynamics of pair fluctuations is relaxational and not propagating, we adopt it hereafter for the sake of definiteness. To make contact with Ref. 5 the prefactor within the AL theory is $\alpha_D = 16e^2\nu^2/D$, the mass term is $m = \gamma^{-1} \log(T/T_c)$, and the characteristic inverse time scale is $\nu \approx \gamma^{-1} \xi_0^2$, where $\gamma = \pi/(8T) = \pi/(8T_c)$ is a characteristic time scale for the damping of pair fluctuations, and ξ_0 is the coherence length (in units of the lattice spacing). We point out that the Eqs. (5) and (6) are valid within a Ginzburg-Landau (GL) context, under quite general conditions, for a generic expression of $\Omega_{\mathbf{q}}$, which may include corrections to the hydrodynamic expression at higher momenta. For instance, in a lattice system, both the factor q^2 in Eq. (5) and the expression for $\Omega_{\mathbf{q}}$ in Eq. (6) are replaced by suitable generalizations that preserve the lattice periodicity.

The suppression of the paraconductivity could, in principle, arise from, e.g., the subleading temperature dependence of the prefactors α_D and from the subleading temperature dependence of the integral in Eq. (6). This analysis was carried out previously,^{21,22} finding power-law dependencies in ϵ . However, the suppression of the paraconductivity at a higher temperature is by far sharper than the one provided by the temperature as the natural cutoff. We are therefore led to discuss the role of an intrinsic cutoff for the momentum integral in Eq. (5).

The analytical development within a BCS derivation of the effective GL theory leads to a natural momentum cutoff $\sim \xi_0^{-1}$ for higher momenta. This cutoff can alternatively be described as the appearance of higher-order terms in the q dependence of $\Omega_{\mathbf{q}}$, beyond the lowest-order term $\sim q^2$. However, neither a strict momentum cutoff $q \leq q_C \sim \xi_0^{-1}$, nor the introduction, e.g., of a q^4 term in $\Omega_{\mathbf{q}}$, account for the observed behavior of the paraconductivity.²³

Based on physical arguments, it was proposed^{18,19} that, rather than a strict cutoff on q , a cutoff should be imposed on the energy (namely, the inverse relaxation time) of the collective pair fluctuations. This cutoff, within the standard BCS-GL theory, takes the form $m + \nu q^2 \leq \xi_0^{-2} T_c$, and leads to a sharper reduction with respect to a strict momentum cutoff. This is easily understood by considering that, away from T_c , m increases, so that a strict cutoff Ω_C on $\Omega_{\mathbf{q}} \approx m + \nu q^2$ amounts to a strict momentum cutoff $q^2 \leq q_C^2 \equiv (\Omega_C - m)/\nu$, which decreases with increasing temperature, thus shrinking the region of momenta that contribute to the paraconductivity. This effect adds on top of the reduction associated with an increasing mass m , and determines a sharper decrease at higher temperatures. However, to fit with this energy cutoff the experimentally determined suppression of the paraconductivity, [Eqs. (1) and (2)] would require a peculiar temperature dependence for Ω_C . In the remaining part of this

section, we analyze the experimental data within an alternative framework, which, although related to the presence of an energy cutoff, rather relies on a model for an effective “density of states” of the collective pair fluctuations. In this model we rely on a smooth energy cutoff, which is temperature independent (but for the subleading temperature dependence of the parameters like γ , ν , and so on), and rather encodes the T^* energy scale. Indeed, we transform the momentum integral into an energy integral, by introducing the effective density of states,²⁴

$$\mathcal{N}_D(\Omega) = \int \frac{d^D \mathbf{q}}{(2\pi)^D} q^2 \delta(\Omega - \Omega_{\mathbf{q}}),$$

for an arbitrary expression of $\Omega_{\mathbf{q}}$ as a function of the momentum. This includes as particular cases, e.g., the effect of a higher-order momentum dependence of $\Omega_{\mathbf{q}}$ with respect to the hydrodynamic q^2 dependence, and/or the cutoff condition $\Omega_{\mathbf{q}} \leq \Omega_C$.

We point out that the minimum value for $\Omega_{\mathbf{q}}$ is m , and therefore

$$\Delta\sigma_D = \alpha_D \int_m^{+\infty} d\Omega \mathcal{N}_D(\Omega) \mathcal{I}(\Omega; T). \quad (7)$$

This equation is our starting point. For the sake of simplicity we discuss the case in which $\mathcal{I}(\Omega_{\mathbf{q}}; T)$ has the leading AL expression⁵ $\mathcal{I}(\Omega_{\mathbf{q}}; T) = T/(2\Omega_{\mathbf{q}}^3)$, but the analysis can be easily extended to the case in which $\mathcal{I}(\Omega; T)$ assumes a more complicated dependence on $\Omega_{\mathbf{q}}$ that interpolates between the low- T ($\Omega_{\mathbf{q}} \gg T$) and the high- T ($\Omega_{\mathbf{q}} \ll T$) regimes.²² This more refined analysis, however, does not significantly change the main results discussed hereafter, and only adds standard subleading temperature dependences, which would not account for the observed suppression of the paraconductivity at higher temperatures, essentially related to the behavior of the effective density of states $\mathcal{N}_D(\Omega)$ at higher energies.

A sharp energy cutoff $\Omega \leq \Omega_C$ translates into a vanishing effective density of states, $\mathcal{N}_D(\Omega) \equiv 0$ for $\Omega > \Omega_C$. We relax this condition, and only assume that the effective density of states vanishes at infinity. More precisely, we write the function to be integrated in Eq. (7) as the derivative with respect to Ω of an auxiliary function, $\alpha_D \mathcal{N}_D(\Omega) \mathcal{I}(\Omega; T) \equiv -\mathcal{F}'_D(\Omega)$, with T taken as a parameter, and assume that $\mathcal{F}_D(\Omega)$ vanishes as $\Omega \rightarrow +\infty$. Then, evidently $\Delta\sigma_D = \mathcal{F}_D(m)$. Recalling that $m = \gamma^{-1}\epsilon$, with $\epsilon \equiv \log(T/T_c)$, we can extract the leading behavior of the effective density of states $\mathcal{N}_D(\Omega)$ at large Ω from the interpolating formula for the paraconductivity proposed in Refs. 2,3, Eq. (1) for $D=2$, and Eq. (2) for $D=3$. Our procedure here is approximate, as it neglects the parametric dependence of the effective density of states on the mass, but captures the main features obtained in Ref. 22 with a more complicated procedure, which allows to disentangle the parametric dependence on the mass. Thus we find

$$\mathcal{N}_D(\Omega) \approx -\frac{1}{\alpha_D \mathcal{I}(\Omega; T)} \frac{d}{d\Omega} \Delta\sigma_D^{\text{exp}}(\epsilon = \gamma\Omega),$$

where the derivative with respect to Ω is taken at constant ϵ_0 .

Therefore, we are led to the conclusion that the spectrum

of the inverse relaxation time for the collective pair fluctuations is cut off exponentially at higher Ω and the characteristic scale for this suppression, $\Omega_0 \equiv \gamma^{-1}\epsilon_0$, increases with decreasing doping, following T^* . The presence of this scale is highly significant and rises the issue of the relation between Cooper pair fluctuations and the pseudogap.²⁵

Since the microscopic interpretation of this finding is beyond the scope of the present work, here we only illustrate two possible interpretations. Coming from high temperatures $T > T^*$, one can identify T^* as the mean-field-like temperature for superconductivity, below which the fluctuations bring the critical temperature down to T_c . The bifurcation between T^* and T_c around optimal doping can be interpreted in a Gaussian GL scheme within a two-gap model.¹³

An alternative interpretation can be proposed, starting from T_c , as the temperature above which pair fluctuations set in. The disappearance of pair fluctuations above T^* can here be interpreted as due to some additional mechanism of strong mixing between, e.g., the particle-particle and the particle-hole channels. In particular, within a scenario with a quantum critical point around optimal doping, the region above T^* is characterized by the presence of quantum-critical fluctuations, which could couple to the superconducting fluctuations, and suppress them. These two possibilities are presently under investigation.²²

III. ASLAMAZOV-LARKIN PARACONDUCTIVITY IN THE PSEUDOGAP REGION

The occurrence of the AL paraconductivity is particularly stringent in two-dimensional systems, where the AL paraconductivity does not contain fitting parameters and takes a universal form with a power-law dependence in ϵ and a definite prefactor [see Eq. (3)]. For this reason, here we concentrate on two-dimensional BSCCO compounds.

The choice of a normal-state conductivity σ_n (or resistivity ρ_n) becomes rather natural around optimal doping, where $\rho_n(T)$ is linear over a wide temperature range. It is in this case that the presence of an AL paraconductivity becomes particularly clear both in $D=2$ (Refs. 6 and 8–11) and $D=3$.^{2,26,27} Remarkably, since the paraconductivity diverges at T_c , the choice of a specific (finite) normal-state conductivity $\sigma_n(T)$ affects little the total conductivity $\sigma(T) = \sigma_n(T) + \Delta\sigma^{\text{AL}}(T)$, and the divergence of $\Delta\sigma^{\text{AL}}$ cannot be missed by a wrong choice of the normal state.²⁸ However, the choice of the correct σ_n becomes crucial for the correct description of the paraconductivity away from T_c . Therefore here we systematically investigate how different normal-state resistivities affect the determination of $\Delta\sigma^{\text{AL}}$ in the resistivity data of Ref. 29. First of all, we notice (see Fig. 2 in Ref. 29) that above a temperature T^* the resistivity is linear in temperature, while it acquires a downward curvature at lower temperatures. Therefore we assume the normal state resistivity ρ_n to be described by a straight line above T^* , while a quadratic curve is adopted below it:

$$\rho_n(T > T^*) = \rho_n^* + A(T - T^*), \quad (8)$$

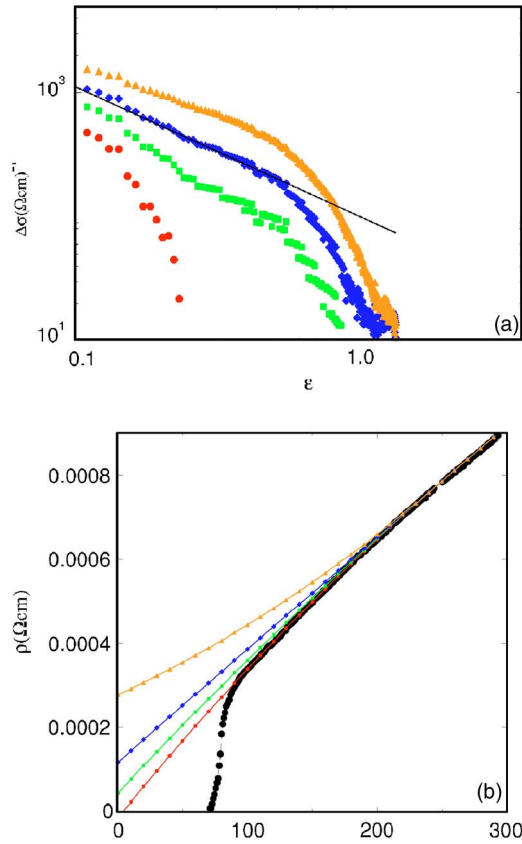


FIG. 1. (Color online) (a) Paraconductivity data, as obtained by taking the different normal-state resistivities. The resistivity data [black circles in Fig. 1(b)] are from Ref. 29 for a BSCCO sample at doping $x=0.217$. The symbols of each set of paraconductivity points corresponds to the symbols of the corresponding normal-state resistivity curves of Fig. 1(b). The solid straight line is the universal two-dimensional AL paraconductivity, Eq. (3), with no adjustable parameter. (b) Resistivity data (black circles) and various hypothetical forms of the normal-state resistivity. All the curves coincide with a straight line above $T^*=250$ K, while are quadratic below it [see Eq. (8)]. The first curve from top has a positive curvature, $B>0$; the second, third, and fourth curve have a negative curvature, $B<0$, which increases in absolute value from top to bottom. The normal-state hypothetical curves are extended to the region below the critical temperature to make them more clearly distinguishable by emphasizing their separation.

$$\rho_n(T < T^*) = \rho_n^* + A(T - T^*) + B(T - T^*)^2,$$

where $\rho_n^* \equiv \rho_n(T=T^*)$.

To explore the effects of assuming different ρ_n we take below T^* the set of parabolae reported in Figs. 1(b) and 2(b).

For each choice of the normal-state resistivity we determine the paraconductivity,

$$\Delta\sigma_{D=2}(T) = \frac{1}{\rho(T)} - \frac{1}{\rho_n(T)},$$

obtaining the data of Figs. 1(a) and 2(a). The solid straight line represents the pure AL paraconductivity in $D=2$, Eq. (3). Rather naturally, if one assumes the normal state to follow closely the resistivity data [the circles in Figs. 1(b) and 2(b)],

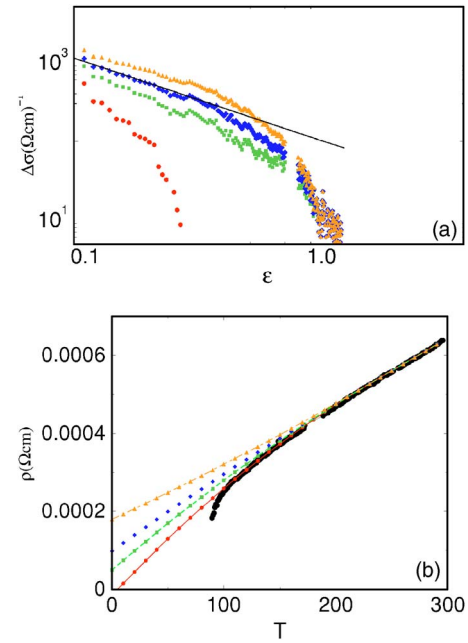


FIG. 2. (Color online) (a) Paraconductivity data, as obtained by taking the different normal-state resistivities. The resistivity data [black circles in Fig. 2(b)] are from Ref. 29 for a BSCCO sample at doping $x=0.22$. The symbols of each set of paraconductivity points corresponds to the symbols of the corresponding normal-state resistivity curves of Fig. 2(b). The solid straight line is the universal two-dimensional AL paraconductivity, Eq. (3) with no adjustable parameter. (b) Resistivity data (black circles) and various hypothetical forms of the normal-state resistivity. All the curves coincide with a straight line above $T^*=220$ K, while are quadratic below it [see Eq. (8)]. The first curve from top has a positive curvature, $B>0$; the second, third, and fourth curve have a negative curvature, $B<0$, which increases in absolute value from top to bottom. The normal-state hypothetical curves are extended to the region below the critical temperature to make them more clearly distinguishable by emphasizing their separation.

there is little space for the paraconductivity contribution, which is rapidly suppressed above T_c . Nevertheless, one can see that approaching T_c the paraconductivity [the circles in Figs. 1(a) and 2(a)] merges with the (diverging) AL contribution. On the other hand, one can adopt the normal-state resistivity with an upward curvature [i.e., with a parameter $B>0$; the triangles in Figs. 1(b) and 2(b)], which emphasizes the difference between the resistivity data and the (supposed) normal-state resistivity. In this case the paraconductivity must be large to bring the large normal-state resistivity down to the observed values. The triangles of the Figs. 1(a) and 2(a) represent this large contribution to the paraconductivity. In this case one sees that $\Delta\sigma_{D=2}(T)$ has the same slope as the pure AL paraconductivity, but has a nearly constant positive offset and is rapidly suppressed around $\epsilon \sim 0.5$, corresponding to $T \sim T^*$. This last effect simply arises from the “perfect” matching of the linear resistivity data with the assumed linear normal state resistivity for $T>T^*$. In between the two limiting cases described above, there is the choice of normal-state resistivities with small (or vanishing) curvature represented by the diamonds in Figs. 1(b) and 2(b). Quite inter-

estingly, one finds that the related paraconductivity closely follows the pure AL behavior, both for the slope and for the absolute (universal) value. This shows that the resistivity data, not only are compatible with a two-dimensional AL behavior near T_c , but also this behavior extends up to T^* provided a (nearly) linear normal-state resistivity is assumed. Also in this case, as soon as the temperature reaches T^* , the paraconductivity rapidly drops.

This behavior is suggestive of the fact that below T^* the resistivity would be linear, were it not for the presence of Gaussian Cooper-pair fluctuations giving AL contributions to the conductivity. These suppress the resistivity below its linear behavior all over the region $T_c < T < T^*$.

IV. CONCLUSIONS

In this paper we critically revisited the paraconductivity data in the cuprates addressing the two main issues: The existence and robustness of the AL paraconductivity, which in underdoped systems survives well above T_c , and the rapid suppression of paraconductivity above T^* . Regarding the second issue, we recast the problem of the cutoff in the pairing collective-mode fluctuations, showing that the rapid suppression of the pairing fluctuations away from T_c can arise from a rapid suppression of the spectral weight of the pair fluctuations above a characteristic energy scale, which directly involves T^* , $\Omega_0 \equiv \gamma^{-1} \log(T^*/T_c)$.

As far as the first issue is concerned, we also find the surprising result that, assuming a (nearly) linear normal-state resistivity, the measured two-dimensional paraconductivity in BSCCO closely follows the pure AL behavior. While we do not have a theory for a linear normal-state resistivity, nor for the persistence of BCS-like pair fluctuations up to T^* , it seems to us that the coincidence (revealed at all dopings up to the optimal one) both for the power-law and the universal prefactors between the extracted paraconductivity and the AL behavior can hardly be casual. This suggests that the temperature dependence of the resistivity in BSCCO is given by a normal-state linear contribution, which is decreased below T^* by the two-dimensional AL paraconductivity. If, as it seems natural, this paraconductivity arises from Gaussian pair fluctuations, our analysis entails that preformed pairs, if any, do not provide a separate additional conductivity channel.

ACKNOWLEDGMENTS

We are indebted to C. Castellani, C. Di Castro, and M. Aprili for interesting discussions and useful comments. S.C. and M.G. acknowledge financial support from MIUR Cofin 2003, Prot. 2003020239_006, and from ESPCI/CNRS, and thank their colleagues at the ESPCI for the warm hospitality.

-
- ¹C. W. Luo, J. Y. Juang, J.-Y. Lin, K. H. Wu, T. M. Uen, and Y. S. Gou, *Phys. Rev. Lett.* **90**, 179703 (2003); B. Leridon, A. Défossez, J. Dumont, J. Lesueur, and J. P. Contour, *Phys. Rev. Lett.* **90**, 179704 (2003).
- ²B. Leridon, A. Défossez, J. Dumont, J. Lesueur, and J. P. Contour *Phys. Rev. Lett.* **87**, 197007 (2001).
- ³B. Leridon, M. Moraguès, J. Lesueur, A. Défossez, J. Dumont, and J. P. Contour, *J. Supercond.* **15**, 409 (2002).
- ⁴For a review see, e.g., J. L. Tallon and J. W. Loram, *Physica C* **349**, 53 (2001).
- ⁵L. G. Aslamazov and A. I. Larkin, *Phys. Lett.* **26A**, 238 (1968); *Sov. Phys. Solid State* **10**, 875 (1968).
- ⁶G. Balestrino, A. Nigro, R. Vaglio, and M. Marinelli, *Phys. Rev. B* **39**, 12264 (1989).
- ⁷G. Balestrino, M. Marinelli, E. Milani, L. Reggiani, R. Vaglio, and A. A. Varlamov, *Phys. Rev. B* **46**, 14919 (1992).
- ⁸W. Lang, G. Heine, W. Kula, and R. Sobolewski, *Phys. Rev. B* **51**, 9180 (1995).
- ⁹M. R. Cimberle, C. Ferdeghini, E. Giannini, D. Marré, M. Putti, A. Siri, F. Federici, and A. Varlamov, *Phys. Rev. B* **55**, R14745 (1997).
- ¹⁰A. A. Varlamov, G. Balestrino, E. Milani, and D. V. Livanov, *Adv. Phys.* **48**, 655 (1999).
- ¹¹S. R. Currás, G. Ferro, M. T. González, M. V. Ramallo, M. Ruibal, J. A. Veira, P. Wagner, and F. Vidal, *Phys. Rev. B* **68**, 094501 (2003).
- ¹²V. B. Geshkenbein, L. B. Ioffe, and A. I. Larkin, *Phys. Rev. B* **55**, 3173 (1997).
- ¹³A. Perali, C. Castellani, C. Di Castro, M. Grilli, E. Piegari, and A. A. Varlamov, *Phys. Rev. B* **62**, R9295 (2000).
- ¹⁴J. Ranninger, J. M. Robin, and M. Eschrig, *Phys. Rev. Lett.* **74**, 4027 (1995); J. Ranninger and J. M. Robin, *Phys. Rev. B* **53**, R11961 (1996), and references therein.
- ¹⁵E. Piegari and S. Caprara, *Phys. Rev. B* **67**, 214503 (2003).
- ¹⁶We point out that an exponential behavior in $\epsilon \equiv \log(T/T_c)$ corresponds to a power law in the temperature T .
- ¹⁷S. Sachdev, *Physica C* **408–410**, 218 (2004).
- ¹⁸F. Vidal, C. Carballeira, S. R. Currás, J. Mosqueira, M. V. Ramallo, J. A. Veira, and J. Viña, *Europhys. Lett.* **59**, 754 (2002), and references therein.
- ¹⁹T. Mishonov and E. Penev, *Int. J. Mod. Phys. B* **14**, 3831 (2000); T. M. Mishonov, G. V. Pachov, I. N. Genchev, L. A. Atanasova, and D. Ch. Damianov, *Phys. Rev. B* **68**, 054525 (2003).
- ²⁰A. Larkin and A. Varlamov, *Theory of Fluctuations in Superconductors* (Clarendon, Oxford, 2005).
- ²¹L. Reggiani, R. Vaglio, and A. A. Varlamov, *Phys. Rev. B* **44**, 9541 (1991).
- ²²S. Caprara, M. Grilli, B. Leridon, and J. Lesueur (unpublished).
- ²³E. Silva, S. Sarti, R. Fastampa, and M. Giura, *Phys. Rev. B* **64**, 144508 (2001).
- ²⁴We refer to $\mathcal{N}_D(\Omega)$ as to an effective density of states, due to the presence of the extra q^2 factor (or of its suitable periodic generalization in a lattice system) in the momentum integral, which renders $\mathcal{N}_D(\Omega)$ not normalized to unity.

- ²⁵This relevance of T^* as a cutoff scale is at variance with the proposal of Ref. 18, where the energy cutoff of pair fluctuations was related to ξ_0 .
- ²⁶P. P. Freitas, C. C. Tsuei, and T. S. Plaskett, *Phys. Rev. B* **36**, 833 (1987).
- ²⁷C. Carballeira, S. R. Currás, J. Viña, J. A. Veira, M. V. Ramallo, and F. Vidal, *Phys. Rev. B* **63**, 144515 (2001).
- ²⁸In principle, one could also investigate the effect of fluctuations in other transport properties under a magnetic field (magnetoresistance and Hall effect). However, since in the physical quantities other than the dc conductivity the fluctuation contributions are nonsingular and nonuniversal, it is much more difficult and ambiguous to identify and separate the normal-state and the fluctuation contributions. This renders such an analysis much less stringent.
- ²⁹T. Watanabe, T. Fujii, and A. Matsuda, *Phys. Rev. Lett.* **79**, 2113 (1997).